

# UC San Diego

## UC San Diego Previously Published Works

### Title

Serum amyloid P (PTX2) attenuates hepatic fibrosis in mice by inhibiting the activation of fibrocytes and HSCs

### Permalink

<https://escholarship.org/uc/item/7qr301n5>

### Journal

Hepatology Communications, 8(11)

### ISSN

2471-254X

### Authors

Cong, Min

Weber, Raquel Carvalho Gontijo

Sakane, Sadatsugu

et al.

### Publication Date

2024

### DOI

10.1097/hc9.0000000000000557

Peer reviewed

## ORIGINAL ARTICLE

OPEN

# Serum amyloid P (PTX2) attenuates hepatic fibrosis in mice by inhibiting the activation of fibrocytes and HSCs

Min Cong<sup>1</sup> | Raquel Carvalho Gontijo Weber<sup>2,3</sup> | Sadatsugu Sakane<sup>2</sup> |  
Vivian Zhang<sup>2,3</sup> | Chunyan Jiang<sup>4</sup> | Kojiro Taura<sup>5,6</sup> | Yuzo Kodama<sup>7</sup> |  
Samuele DeMinicis<sup>8</sup> | Souradipta Ganguly<sup>2</sup> | David Brafman<sup>9</sup> | Shu Chien<sup>10</sup> |  
Michael Kramer<sup>11</sup> | Mark Luper<sup>12</sup> | David A. Brenner<sup>2,13</sup> | Jun Xu<sup>2,14</sup> |  
Tatiana Kisseleva<sup>2</sup>

<sup>1</sup>Liver Research Center, Beijing Friendship Hospital, Capital Medical University, Beijing, China

<sup>2</sup>Department of Medicine, University of California, San Diego, La Jolla, California, USA

<sup>3</sup>Department of Surgery, University of California, San Diego, La Jolla, California, USA

<sup>4</sup>Department of Internal Medicine and Geriatrics, Beijing Friendship Hospital, Capital Medical University, Beijing, China

<sup>5</sup>Division of Hepatobiliary-Pancreatic Surgery and Transplantation, Department of Surgery, Graduate School of Medicine, Kyoto University, Kyoto, Japan

<sup>6</sup>Department of Gastroenterological Surgery and Oncology, Kitano Hospital Medical Research Institute, Osaka, Japan

<sup>7</sup>Division of Gastroenterology, Department of Internal Medicine, Kobe University Graduate School of Medicine, Kobe, Japan

<sup>8</sup>Department of Gastroenterology, Augusto Murri Hospital, Polytechnic University of Marche, Ancona, Italy

<sup>9</sup>School of Biological and Health Systems Engineering, Arizona State University, Tempe, Arizona, USA

<sup>10</sup>Jacobs School of Engineering, University of California, San Diego, La Jolla, California, USA

<sup>11</sup>Quanta Therapeutics Inc., Radnor Life Sciences Center, Philadelphia, Pennsylvania, USA

<sup>12</sup>Adverum Biotechnologies, Inc. Redwoods, California, USA

<sup>13</sup>Sanford Burnham Prebys, La Jolla, California, USA

<sup>14</sup>Gilead Sciences, Foster City, California, USA

## Correspondence

Min Cong, Liver Research Center, Beijing Friendship Hospital, Capital Medical University, 95 Yong-an Road, XiCheng, Beijing 100050, China.  
Email: [maomao0623@sina.com](mailto:maomao0623@sina.com)

Jun Xu, Gilead Sciences, 333 Lakeside Dr, Foster City, CA 94404, USA.  
Email: [Jun.Xun@gilead.com](mailto:Jun.Xun@gilead.com)

Tatiana Kisseleva, Department of Medicine, University of California, San Diego, 9500 Gilman Drive, #0063, La Jolla, CA 92093, USA.  
Email: [tkisseleva@health.ucsd.edu](mailto:tkisseleva@health.ucsd.edu)

## Abstract

**Background:** Liver fibrosis is caused by chronic toxic or cholestatic liver injury. Fibrosis results from the recruitment of myeloid cells into the injured liver, the release of inflammatory and fibrogenic cytokines, and the activation of myofibroblasts, which secrete extracellular matrix, mostly collagen type I. Hepatic myofibroblasts originate from liver-resident mesenchymal cells, including HSCs and bone marrow-derived CD45<sup>+</sup> collagen type I<sup>+</sup> expressing fibrocytes. Recombinant human serum amyloid P (hSAP), a natural inhibitor of fibrocyte activation into myofibroblasts, was shown to

**Abbreviations:** aHSCs, activated hepatic stellate cell/myofibroblasts; BDL, bile duct ligation; BM, bone marrow; CCl<sub>4</sub>, carbon tetrachloride; ECM, extracellular matrix; FBS, fetal bovine serum; hSAP, recombinant human serum amyloid P (Pentraxin 2); NPC, non-parenchymal fraction; PTX2, Pentraxin 2; qHSCs, quiescent HSCs; RT-PCR, reverse transcription polymerase chain reaction; TIMP1, tissue inhibitor of metalloproteinases 1.

Supplemental Digital Content is available for this article. Direct URL citations are provided in the HTML and PDF versions of this article on the journal's website, [www.hepcommjournal.com](http://www.hepcommjournal.com).

This is an open access article distributed under the terms of the Creative Commons Attribution-Non Commercial-No Derivatives License 4.0 (CCBY-NC-ND), where it is permissible to download and share the work provided it is properly cited. The work cannot be changed in any way or used commercially without permission from the journal.

Copyright © 2024 The Author(s). Published by Wolters Kluwer Health, Inc. on behalf of the American Association for the Study of Liver Diseases.

ameliorate experimental renal, lung, skin, and cardiac fibrosis. We investigated if hSAP can ameliorate the development of liver fibrosis of different etiologies.

**Methods:** Reporter Collagen- $\alpha(1)$ I-GFP mice were subjected to cholestatic liver injury (by ligation of the common bile duct) or toxic liver injury (by carbon tetrachloride administration) and treated prophylactically or therapeutically with hSAP (12.5  $\mu$ g/g). Primary cultures of mouse fibrocytes and HSCs were stimulated to activate with or without incubation with hSAP.

**Results:** We demonstrate that treatment with hSAP suppressed hepatic fibrosis by  $\approx$ 50% through dual mechanisms. hSAP prevented the recruitment of fibrocytes into the injured liver and their differentiation into myofibroblasts. Remarkably, hSAP also inhibited the activation of HSCs into myofibroblasts.

**Conclusions:** Since HSCs serve as a major source of collagen type I-producing myofibroblasts and fibrocytes stimulate fibrosis, hSAP may become part of the therapy of liver fibrosis of different etiologies.

**Keywords:** fibrocytes, HSCs, liver fibrosis, myofibroblasts

## INTRODUCTION

Hepatic fibrosis develops in response to chronic hepatotoxic or cholestatic liver injury and is characterized by the deposition of extracellular matrix (ECM) proteins, forming a fibrous scar. Hepatotoxic injury is caused by HBV or HCV infections, metabolic dysfunction-associated steatohepatitis, and alcohol-associated liver disease.<sup>[1]</sup> Cholestatic injury is caused by obstruction to bile flow, such as in primary and secondary biliary cholangitis, primary sclerosing cholangitis, and biliary atresia. Development of liver fibrosis is associated with chronic hepatocyte damage and death, increased intestinal permeability, recruitment and activation of liver-resident (KCs) and bone marrow (BM)-derived myeloid cells, release of inflammatory (TNF, IL-1 $\beta$ , IL-6, CCL2, and CCL5) and profibrogenic (TGF $\beta$ 1, CTGF, and PTGF) cytokines and chemokines,<sup>[1]</sup> and activation of collagen type I-producing myofibroblasts. Myofibroblasts are not present in the normal liver. Liver-resident activated hepatic stellate cells (aHSCs) are the major source of myofibroblasts in the fibrotic liver, while activated portal fibroblasts contribute mainly to cholestatic liver fibrosis. Quiescent HSCs and PFs activate into myofibroblasts in response to chronic liver injury.<sup>[2]</sup>

In addition to liver-resident mesenchymal cells, myofibroblasts can also originate from the BM-derived fibrocytes, a population of CD45<sup>+</sup> and collagen type I<sup>+</sup> expressing cells, which are recruited to the damaged liver.<sup>[3]</sup> Fibrocytes are implicated in the pathogenesis of fibrogenic diseases in the lungs, skin, kidneys, and liver,<sup>[3–6]</sup> where they have been reported to contribute

up to 25% of collagen-producing cells in specific pathological states.<sup>[7]</sup> While the role of fibrocytes in the pathogenesis of lung and kidney fibrosis has been extensively studied, the functions of fibrocytes in liver fibrosis remain unresolved.

First described by Bucala and colleagues, fibrocytes represent a unique population of myeloid cells expressing hematopoietic (CD45, CD34, MHCII, CD11b, Gr1, Ly6c, CD54, CD80, CD86, CCR2, CCR1, and CCR5) and fibroblast-like (collagen type I, fibronectin, and vimentin) markers.<sup>[3,8]</sup> Under physiological conditions, fibrocytes reside in the BM (comprising 0.1% of mononuclear cells). In response to liver injury, fibrocytes proliferate, egress the BM, and migrate to the spleen<sup>[9]</sup> (which serves as a reservoir of immature BM-derived fibrocytes<sup>[9,10]</sup>) and the damaged liver. In the liver, the majority of fibrocytes acquire proinflammatory myeloid phenotype, while some fibrocytes downregulate the expression of hematopoietic markers and differentiate into  $\alpha$ -SMA<sup>+</sup>Col $\alpha$ 1( $\alpha$ )<sup>+</sup> myofibroblasts<sup>[3]</sup> and contribute to the populations of hepatic myofibroblasts.

Serum amyloid P (SAP, also known as Pentraxin 2 [PTX2]; *APCS* gene) is a natural inhibitor of fibrocyte differentiation into myofibroblasts, which was implicated in the regulation of tissue remodeling. Human SAP has 51% sequence homology with C-reactive protein and PTX3 (a cytokine-modulated molecule).<sup>[11]</sup> Human and mouse SAP are evolutionarily conserved.<sup>[12]</sup> Therefore, recombinant human SAP (hSAP) was shown to inhibit monocyte differentiation into fibrocytes in both species.<sup>[13]</sup> Administration of hSAP ameliorated the development of experimental fibrosis in several

organs,<sup>[11]</sup> including pulmonary fibrosis.<sup>[14,15]</sup> Although a phase III trial of rhPTX-2 (NCT04552899) in patients with idiopathic pulmonary fibrosis failed to achieve its primary endpoint, targeting fibrocytes in other fibrotic diseases might uncover therapeutic potential of hSAP (<https://classic.clinicaltrials.gov/ct2/show/NCT04552899>).

This study investigates the potential therapeutic effects of hSAP on the development and treatment of liver fibrosis in mice subjected to chronic cholestatic (bile duct ligation, BDL) or toxic (carbon tetrachloride, CCl<sub>4</sub>) liver injury. Here we report that administration of hSAP inhibited inflammation and liver fibrosis of both etiologies. Corroborating the *in vivo* studies, hSAP exerted its functions by simultaneously targeting BM-derived fibrocytes and liver-resident HSCs and preventing fibrocyte and HSC activation into myofibroblasts.

## METHODS

### Mice

Wild-type C57BL/6 mice (males and females) were purchased from The Jackson Laboratory. Transgenic Col-GFP mice, which express *gfp* under the control of *collagen-α1(I)* promoter/enhancer, were previously characterized.<sup>[16]</sup> Col-GFP mice underwent BDL or administration of CCl<sub>4</sub>. Mice were maintained at the University of California San Diego under specific pathogen-free conditions (IACUC, S07088).

### BDL-induced liver injury

Mice (males and females, 8 weeks old, *n* = 8–10/group) were anesthetized with ketamine and xylazine. After midline laparotomy, the common bile duct was ligated twice with 6-0 silk sutures, and the abdomen was closed. Sham operation was performed similarly, except that the bile duct was not ligated. Animals were sacrificed 17 days after BDL.<sup>[17]</sup>

### CCl<sub>4</sub>-induced liver injury

Mice (males and females, 8 weeks old, *n* = 8–10/group) were administered CCl<sub>4</sub> (Sigma-Aldrich; 0.5 μL/g body weight in corn oil) or vehicle (corn oil) *i.p.* at a dose of twice per week for 6 weeks, for a total of 12 injections.<sup>[17]</sup>

### Administration of hSAP

The optimal concentration of hSAP was determined as described in Supplemental Materials (Supplemental Methods, <http://links.lww.com/HC9/B58> and Supplemental

Figures S1–S3, <http://links.lww.com/HC9/B59>). We determined that 12.5 μg/g of hSAP (a gift from Promedior Inc.) is the minimal nontoxic concentration that exerts a significant effect on inhibition of liver injury, inflammation, and fibrosis in BDL (17 days)-operated mice. For the BDL model, mice were injected *i.p.* with either 12.5 μg/g of hSAP or an equal volume of PBS the day after BDL surgery and on days 3, 5, 7, 9, 11, 13, and 15. For the CCl<sub>4</sub> model, consecutive 4 days dosing (12.5 μg/g, *i.p.*) of hSAP or PBS was started 1 day after CCl<sub>4</sub> administration, followed by twice a week hSAP administration for the duration of liver injury. For therapeutic treatment, consecutive 4 days dosing (12.5 μg/g, *i.p.*) of hSAP or PBS was started on day 10 after CCl<sub>4</sub> administration, followed by twice a week hSAP administration for the duration of liver injury.

### Histological examination

Fixed livers (4% paraformaldehyde optimal cutting temperature, 30% sucrose) were embedded in OCT. Cryosections were stained with hematoxylin and eosin, and Sirius red staining with anti-α-SMA Ab (1:200, Abcam), anti-Desmin Ab (1:300, Thermo), and anti-F4/80 Ab (1:200, eBioscience), followed by Alexa Fluor 594-conjugated secondary Abs. Images (5–7 random fields) were taken using an Olympus microscope and quantified using ImageJ software.

### Quantitative Reverse Transcription Polymerase Chain Reaction

RNA was isolated from livers or isolated HSCs using TRIzol (Invitrogen) followed by an RNeasy kit (Qiagen). Quantitative reverse transcription polymerase chain reaction was performed using an ABI 7000 sequence detection system (Applied Biosystems). Quantification was performed by comparing the Ct values of each sample with a standard curve and normalization to 18s.

### Isolation and activation of GFP<sup>+</sup> cells from the livers, BMs, and spleens of CCl<sub>4</sub>-injured Col-GFP mice

Liver cells were isolated from CCl<sub>4</sub>-injured Col-GFP male and female mice using pronase E (EMD) and collagenase D (Roche Diagnostics) perfusion (perfusion solution: 140 mM NaCl, 5 mM KCl, 0.7 mM NaH<sub>2</sub>PO<sub>4</sub>, 0.8 mM Na<sub>2</sub>PO<sub>4</sub>, 10 mM HEPES, 3 mM NaCO<sub>3</sub>, 4 mM CaCl<sub>2</sub>, and pH 7.4), followed by gradient centrifugation to obtain nonparenchymal fraction (non-parenchymal fraction [NPC]).<sup>[18]</sup> BM and spleenocytes were isolated from CCl<sub>4</sub>-injured Col-GFP male and female mice as

described.<sup>[9]</sup> Total liver fraction, NPCs, BM, and splenocytes were analyzed for the presence of CD45<sup>+</sup>GFP<sup>+</sup> fibrocytes using a FACScan flow cytometer (Becton-Dickinson).<sup>[9]</sup> CD45<sup>+</sup>GFP<sup>+</sup> fibrocytes were purified from liver NPCs using cell sorting. Briefly, liver NPCs were stained with PE-conjugated anti-CD45 antibodies (BD Biosciences) and then sort purified. Obtained CD45<sup>+</sup>GFP<sup>+</sup> cells ( $5 \times 10^5$  cells per well) were plated on the plastic tissue culture dishes (overnight), then pretreated with  $\pm$  hSAP (20  $\mu$ g/mL in PBS) for 15 minutes, and stimulated  $\pm$  TGF- $\beta$ 1 (2 ng/mL; RD Systems) for 48 hours.

## Isolation and activation of mouse HSCs

Primary HSCs were purified from the livers of CCl<sub>4</sub>-injured Col-GFP male and female mice by pronase/collagenase perfusion followed by gradient centrifugation (8.2% Nycodenz; Accurate Chemical and Scientific Corp.).<sup>[18]</sup> Freshly isolated HSCs were cultured on rat collagen type I (Enzo Life Sciences)-coated glass tissue dishes for 18 hours, then stimulated with TGF $\beta$ 1 (2 ng/mL or vehicle) in the presence or absence of different concentrations of hSAP (20, 30, and 40  $\mu$ g/mL) for 72 hours. Alternatively, isolated HSCs were cultured on platforms containing ECM1 (composed of Fibronectin + Col1a1) or ECM2 (composed of Fibronectin + Col1a3) in DMEM +1%, or +10% fetal bovine serum (FBS)  $\pm$  40  $\mu$ g/mL hSAP for 6 days, as described.<sup>[19]</sup> Invitrogen Hoechst (Invitrogen) staining was performed to visualize nuclei in HSCs. The activation of HSCs was detected by the reporter Col-GFP expression using fluorescent microscopy. Bright-field images were taken to visualize the number of cells. Cellular arrays (triplicates) were imaged at the end of the sixth day.

## Bone marrow transplantation

To generate fibrocyte-specific mice, BM from transgenic Col-GFP or  $\beta$ -actin-RFP male mice was transplanted into lethally irradiated recipient (1200 rad) wild-type male C57BL6 mice (2 mo old, males and females). Chimeric  $\beta$ -actin-RFP $\rightarrow$ wt mice were used 2 months after bone marrow transplantation to determine the efficiency of BM reconstitution as described.<sup>[9]</sup> Chimeric  $\beta$ -actin-RFP $\rightarrow$ wt mice recuperated for 2 months and were subjected to liver injury.

## Human hepatocyte and qHSC cultures

Human liver cells were isolated as described.<sup>[18,20]</sup> Primary human qHSCs (passage 3 [P3],  $5 \times 10^4$  cells/well/6-well plate) were serum starved for 24 hours, then pretreated with  $\pm$  hSAP for 15 minutes (1  $\mu$ g/mL, Abcam) and stimulated  $\pm$  TGF $\beta$  (5 ng/mL) for 18 hours,

harvested and analyzed using quantitative reverse transcription polymerase chain reaction (normalized to 18s) for the expression of fibrogenic genes. Human hepatocytes ( $1 \times 10^6$  cells/well/6-well plate) were cultured in the presence or absence of different concentrations of hSAP (100 ng/mL, 500 ng/mL, or 1  $\mu$ g/mL, Abcam) for 18 hours. The effect of hSAP on hepatocyte viability and basal functions was tested using WST-1 assay (water-soluble tetrazolium salt assay, Abcam) and Trypan Blue (Corning) staining to measure cell viability, albumin expression using quantitative reverse transcription polymerase chain reaction (normalized to HPRT), and ELISA to detect secreted albumin (Abcam). Differences in hSAP concentrations used in mouse HSCs and human HSCs are attributed to manufacturing protocols designed by Promedior versus Abcam, and/or efficiency of hSAP binding to human HSCs (vs. mouse HSCs).

## Statistical analysis

The Student *t* test was used to determine statistical significance between groups, unpaired Student *t* test, and a 1-way ANOVA were performed to analyze the variance among groups of sham and difference doses of hSAP in the in vitro experiments. GraphPad PRISM 7.0 software was used for the statistical analysis. *p* value <0.05 was considered statistically significant.

## RESULTS

### Study outline

The development of liver fibrosis is associated with the depletion of SAP levels in humans and mice.<sup>[21]</sup> Here, we investigate if i.p. delivery of the recombinant human SAP (hSAP) can prevent or suppress the progression of liver fibrosis of different etiologies in mice. Specifically, the role of hSAP in the differentiation and activation of fibrocyte-derived versus liver-resident myofibroblasts was assessed. For this purpose, Col-GFP reporter mice<sup>[16]</sup> (C57BL6, males and females, 8 weeks old, *n* = 10/group), which express GFP in all collagen type I-producing cells, were subjected to cholestatic or toxic liver injury and treated with hSAP (or vehicle). The effect of prophylactic and therapeutic treatment with hSAP on the development of liver fibrosis was evaluated.

### Prophylactic administration of human hSAP prevented the development of cholestatic liver fibrosis in mice

Cholestatic fibrosis was induced in Col-GFP mice by ligation of the common bile duct for 17 days. The





was associated with increased inflammation (hematoxylin and eosin), an influx of BM-derived myeloid cells into the injured liver, and marked proliferation and activation of HSCs, as visualized by increased positive area of staining for F4/80 ( $\approx$ 4 fold), Desmin and  $\alpha$ SMA ( $\approx$ 6 fold), respectively (compared to sham-operated Col-GFP mice, [Figure 1A](#)).

In turn, the administration of hSAP (12.5  $\mu$ g/g, i.p., every second day) throughout the duration of cholestatic injury suppressed liver damage, inflammation (as shown by  $\downarrow 40 \pm 0.6\%$  reduction of positive area of F4/80 staining in hSAP-treated BDL mice vs. PBS-treated mice, 100%), suppressed HSC activation ( $\downarrow 46 \pm 0.6\%$  of Desmin and  $\downarrow 41 \pm 0.6\%$   $\alpha$ -SMA positive area, [Figure 1A](#),  $p < 0.01$ ), and liver fibrosis ( $\downarrow 43 \pm 1.2\%$  Col-GFP and  $\downarrow 42 \pm 0.8\%$  Sirius red positive area versus BDL-operated Col-GFP mice treated with PBS, 100%, [Figure 1A](#)). Furthermore, mRNA expression of inflammatory and fibrogenic markers, TGF $\beta$ 1, IL-1 $\beta$ , and IL-6, was reduced by  $\downarrow 39 \pm 3\%$ , and CD68 by  $\downarrow 55 \pm 2\%$  in hSAP-treated BDL mice, and correlated with  $\downarrow 41 \pm 3\%$  downregulation of Collagen  $\alpha$ 1(I),  $\alpha$ SMA, and tissue inhibitor of metalloproteinases 1 (TIMP1) mRNA, demonstrating that prophylactic treatment of BDL-injured mice with hSAP prevents the development of cholestatic fibrosis ([Figure 1B](#)).

### Prophylactic administration of hSAP ameliorated the development of CCl<sub>4</sub>-induced liver fibrosis in mice

To investigate the effect of hSAP on the pathogenesis of toxic liver fibrosis, Col-GFP mice were subjected to CCl<sub>4</sub>-induced liver injury (i.p., 12 injections in 6 wk) and simultaneously treated with hSAP (12.5  $\mu$ g/g, i.p., once a week, 6 wk) or PBS ( $n = 8$ –10/group). In comparison with control mice (that received corn oil, i.p.), CCl<sub>4</sub>-injured mice developed severe liver injury, inflammation, bridging septal fibrosis (hematoxylin and eosin), and upregulated expression of inflammatory and fibrogenic genes ([Figure 2A](#)).

hSAP-treated Col-GFP mice had blunted CCl<sub>4</sub>-induced liver injury. The Sirius Red and Col-GFP-positive areas were reduced in hSAP-treated CCl<sub>4</sub>-Col-GFP mice ( $\downarrow 70 \pm 2\%$  and  $\downarrow 57 \pm 0.8\%$ , respectively, vs. 100% in PBS-treated mice). This effect was associated with a reduced influx of inflammatory F4/80<sup>+</sup> myeloid cells by  $\downarrow 67 \pm 4\%$  ([Figure 2A](#)), with downregulation of TGF $\beta$ 1, IL-1 $\beta$ , IL-6, and TNF $\alpha$  mRNA by  $\downarrow 58 \pm 5\%$ , and decreased activation of Desmin<sup>+</sup> and  $\alpha$ SMA<sup>+</sup> myofibroblasts ([Figure 2B](#)). Expression of fibrogenic mRNAs Collagen  $\alpha$ 1(I),  $\alpha$ SMA, and TIMP1 was also downregulated by  $\downarrow 53 \pm 6\%$ . Our data suggested that the administration of hSAP decreased the development of liver fibrosis of different etiologies.

### Therapeutic administration of hSAP-suppressed CCl<sub>4</sub>-induced liver fibrosis in mice

hSAP (or PBS) was therapeutically administered to CCl<sub>4</sub>-treated Col-GFP mice, for example, 10 days after the onset of CCl<sub>4</sub> injury ([Figure 3A](#)). Delayed administration of hSAP effectively attenuated the development of hepatic inflammation and fibrosis in CCl<sub>4</sub>-Col-GFP mice ([Figure 3B](#)). We observed that the positive area of Sirius Red,  $\alpha$ SMA, and Desmin staining was reduced by  $\approx$ 46  $\pm$  5% in the livers of hSAP-treated CCl<sub>4</sub>-Col-GFP mice ([Figure 3B](#)) that correlated with low levels of hydroxyproline ([Figure 3C](#)), Col- $\alpha$ 1(I),  $\alpha$ SMA, and TIMP1 mRNA ([Figure 3D](#)), indicating that hSAP can be used for the treatment of liver fibrosis.

### hSAP suppressed the influx of fibrocytes into the livers of CCl<sub>4</sub>-injured BM chimeric Col-GFP $\rightarrow$ wt mice

To gain insight into the mechanism by which hSAP exerts its antifibrotic effect, fibrocyte-specific BM chimeric mice were generated by transplanting reporter Col-GFP BM (to visualize fibrocytes) into lethally irradiated wt male and female mice as described<sup>[9]</sup> ([Figure 4A](#)). Control mice were transplanted with  $\beta$ -actin-RFP BM to estimate the efficiency of BM reconstitution. Mice recuperated for 2 months, and the high efficiency of BM reconstitution was confirmed by the presence of >94% of donor  $\beta$ -actin-RFP<sup>+</sup> cells in the BM of recipient mice (not shown). Chimeric Col-GFP $\rightarrow$ wt mice ( $n = 10$ /group) were subjected to CCl<sub>4</sub> (12 i.p. injections for 6 wk) and were therapeutically (with 10 days delay) treated with  $\pm$  hSAP (12.5  $\mu$ g/g, i.p., once a week, throughout the remaining CCl<sub>4</sub> injury). Histological examination revealed that BM-derived Col-GFP<sup>+</sup> fibrocytes migrated to the injured livers of CCl<sub>4</sub> Col-GFP $\rightarrow$ wt mice ([Figure 4A](#)). The majority of GFP<sup>+</sup> cells retained a round shape, and only a fraction of GFP<sup>+</sup> cells resembled myofibroblasts (shown with arrow). Therapeutic administration of hSAP significantly reduced the number of GFP<sup>+</sup> fibrocytes homing to the damaged liver and spleen, which serves as a reservoir of BM-derived fibrocytes (by  $\approx$ 62  $\pm$  5% and by  $\approx$ 50  $\pm$  3%, respectively, compared to the total number GFP<sup>+</sup> cells in the livers and spleens of PBS-treated CCl<sub>4</sub> Col-GFP $\rightarrow$ wt mice, [Figures 4A, B](#)). Surprisingly, the number of Col-GFP<sup>+</sup> cells was also reduced in the BM of hSAP-treated CCl<sub>4</sub> Col-GFP $\rightarrow$ wt mice ([Figure 4B](#)), suggesting that hSAP may suppress differentiation of BM-resident myeloid progenitors into fibrocytes. Moreover, the development of liver fibrosis was suppressed in hSAP-treated CCl<sub>4</sub> Col-GFP $\rightarrow$ wt mice, as shown by reduced area of Sirius Red staining (by  $\downarrow 57 \pm 3\%$ , [Figures 4A, C](#)), and expression of Col- $\alpha$ 1(I) mRNA ( $\downarrow 47 \pm 5\%$ , [Figure 4C](#)).



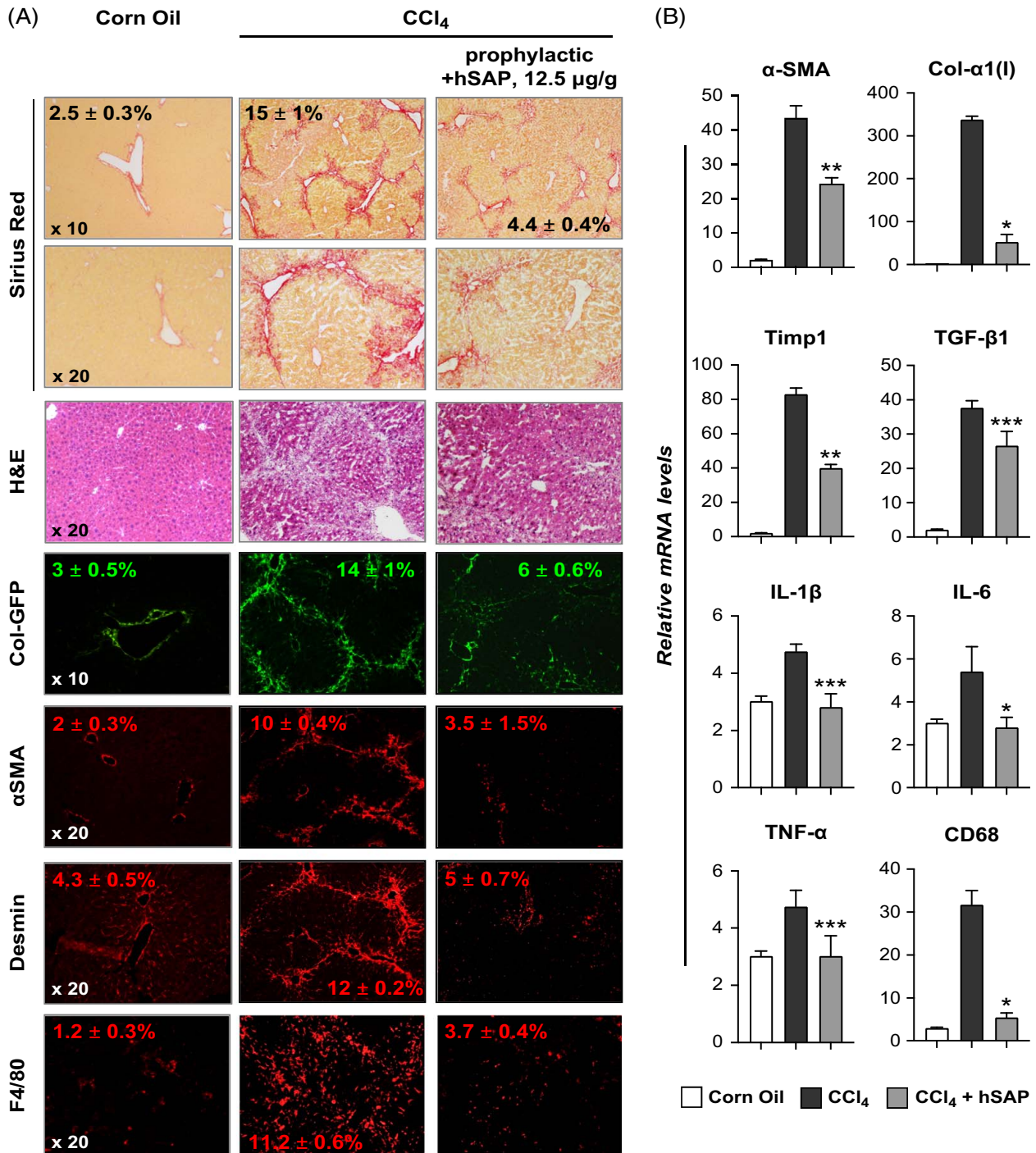


**FIGURE 2** Prophylactic administration of hSAP suppresses CCl<sub>4</sub>-induced liver fibrosis. (A) Livers from corn oil- or CCl<sub>4</sub>-injured ± hSAP-treated Col-GFP mice (n = 8–10/group) were analyzed by immunohistochemistry. Col-α1(I)<sup>+</sup> cells were visualized by the expression of GFP. Positive area was calculated as a percent. Representative images are ×10 or ×20 magnification. (B) Expression of fibrogenic and inflammatory genes was analyzed using quantitative RT-PCR (mRNA levels normalized by 18s). Data are mean ± SD; \**p* < 0.05, \*\**p* < 0.03, \*\*\**p* < 0.01, unpaired Student *t* test, one-way ANOVA. Abbreviations: CCl<sub>4</sub>, carbon tetrachloride; hSAP, human serum amyloid P; RT-PCR, reverse transcription polymerase chain reaction.

### hSAP prevents fibrocyte differentiation into myfibroblasts

Fibrocytes have been implicated in the pathogenesis of liver fibrosis by differentiating into fibrogenic myfibroblasts.<sup>[11]</sup> To test whether hSAP could

suppress fibrocyte differentiation, CD45<sup>+</sup>Col-GFP<sup>+</sup> fibrocytes were isolated from the livers of CCl<sub>4</sub> Col-GFP mice, plated and stimulated with TGF-β1 in the presence or absence of hSAP (20 µg/mL, Figure 4E). After 48 hours of TGF-β1 (2 ng/mL) stimulation, fibrocytes downregulated expression of CD45 hematopoietic marker and acquired



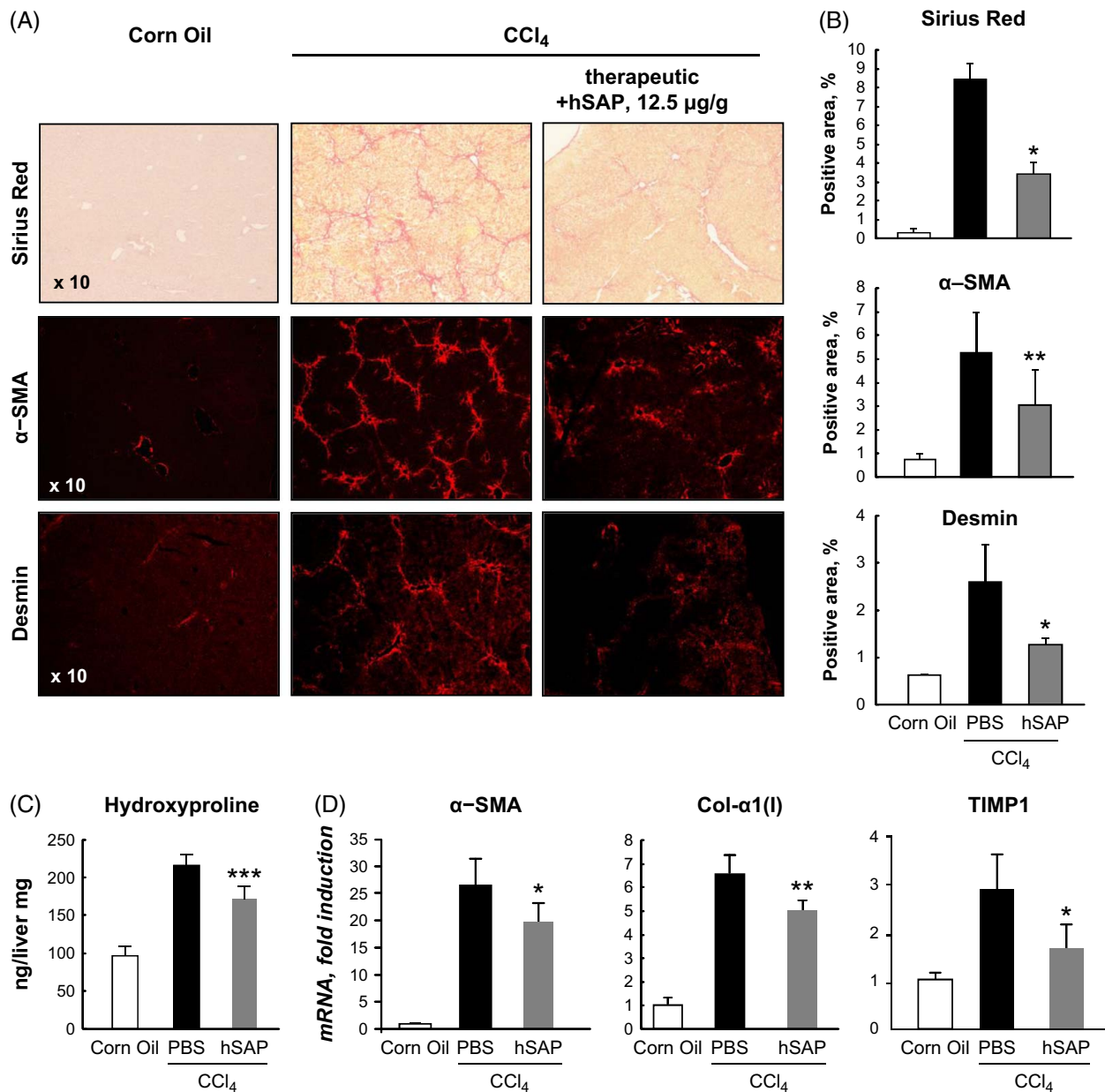


**FIGURE 3** Therapeutic administration of hSAP ameliorates CCl<sub>4</sub>-induced liver fibrosis. (A) Livers from corn oil- or CCl<sub>4</sub>-injured ± hSAP-treated wt mice (n = 8–10/group) were stained with Sirius Red, anti-α-SMA, and anti-Desmin Abs and analyzed by immunohistochemistry. Representative images are taken using ×10 magnification. (B) Positive area was calculated as a percent. (C) The hydroxyproline content was measured in the livers from corn oil or CCl<sub>4</sub>-injured ± hSAP-treated wt mice. (D) Expression of fibrogenic α-SMA, Col-α1(I), and TIMP1 mRNA was analyzed using quantitative RT-PCR (mRNA levels normalized by 18s). Data are mean ± SD; \**p* < 0.05, \*\**p* < 0.03, \*\*\**p* < 0.01, unpaired Student *t* test, one-way ANOVA. Abbreviations: CCl<sub>4</sub>, carbon tetrachloride; hSAP, human serum amyloid P; RT-PCR, reverse transcription polymerase chain reaction; TIMP1, tissue inhibitor of metalloproteinases 1.

stellate-like shape and stress fibers characteristic of myofibroblasts. In turn, fibrocyte differentiation into myofibroblasts was strongly suppressed by hSAP (Figure 4E).

### hSAP effect is not limited to the inhibition of fibrocyte activation and differentiation

Although a relatively small number of fibrocytes (Figures 4A, B) compared to all Col-GFP<sup>+</sup> cells

contribute to collagen type I+ myofibroblasts in the livers of CCl<sub>4</sub> Col-GFP→wt mice, treatment with hSAP resulted in >60% inhibition of toxic liver fibrosis in these mice (Figure 2). In addition, purified fibrocytes expressed significantly less collagen type I mRNA compared to purified aHSCs (Figure 5A), suggesting that hSAP might also target other mesenchymal cells in the liver. The inhibitory effect of hSAP on the development of inflammatory responses in fibrocytes and other myeloid cells has been previously

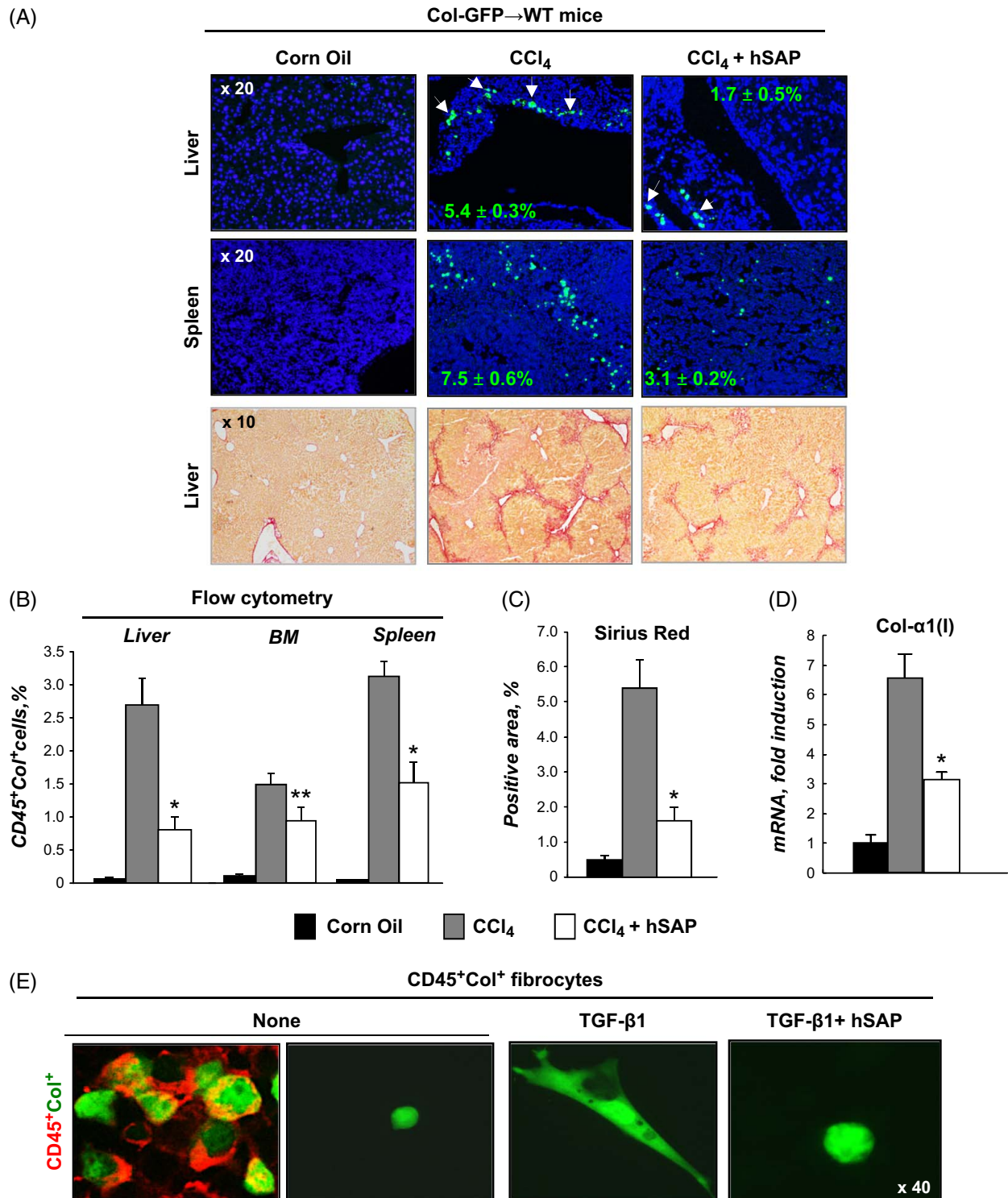


**FIGURE 4** Human SAP inhibits differentiation of fibrocytes into myfibroblasts. (A) Livers from corn oil or CCl<sub>4</sub>-injured ± hSAP-treated BM chimeric Col-GFP→wt mice were analyzed by fluorescent microscopy for the presence of GFP<sup>+</sup> fibrocytes. Livers were stained with Sirius Red to assess liver fibrosis in these mice. Representative images are ×10 or ×20 magnification. (B) The number of CD45<sup>+</sup>Col<sup>+</sup> fibrocytes in the livers, BM, and spleens of corn oil- or CCl<sub>4</sub>-injured ± hSAP-treated BM chimeric Col-GFP→wt mice were detected using flow cytometry. (C) Positive area of Sirius Red staining livers of corn oil or CCl<sub>4</sub>-injured ± hSAP-treated BM chimeric Col-GFP→wt mice was calculated as a percent. (D) Expression of Col-α1(I) mRNA was analyzed using quantitative RT-PCR (mRNA levels normalized by 18s). (E) In vitro differentiation of CD45<sup>+</sup>Col<sup>+</sup> fibrocytes into myfibroblasts in response to TGF-β1 ± hSAP treatment. (F) In vitro differentiation of CD45<sup>+</sup>Col<sup>+</sup> fibrocytes into myfibroblasts in response to TGF-β1 ± hSAP treatment. Representative images of 3 experiments are taken using ×40 magnification. Representative images are taken using ×40 magnification. Data are mean ± SD; \**p* < 0.05, \*\**p* < 0.03, \*\*\**p* < 0.01, unpaired Student *t* test, one-way ANOVA. Abbreviations: BM, bone marrow; CCl<sub>4</sub>, carbon tetrachloride; hSAP, human serum amyloid P; RT-PCR, reverse transcription polymerase chain reaction; SAP, serum amyloid P.

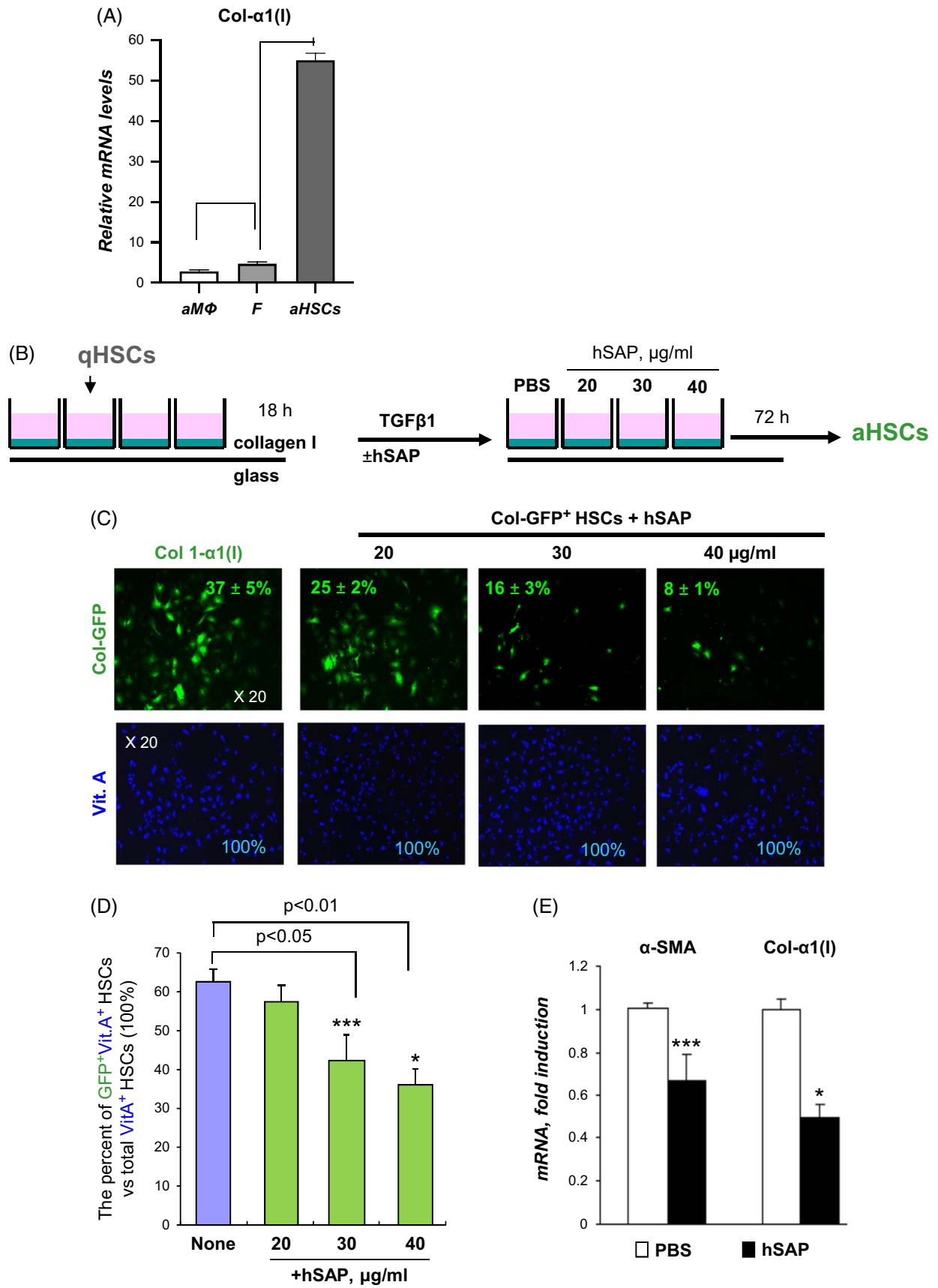


**FIGURE 5** TGF $\beta$ 1 induced in vitro activation of qHSCs into myofibroblasts is blocked in the presence of hSAP in a dose-dependent manner. (A) Expression of Col- $\alpha$ 1(I) mRNA was analyzed using quantitative RT-PCR in macrophages (M $\Phi$ ), fibrocytes, and aHSCs isolated from livers of CCl $_4$ -injured Col-GFP mice as described.<sup>[9]</sup> On average, expression of Col- $\alpha$ 1(I) mRNA in fibrocytes was 2-fold increased versus macrophages but was 14-fold reduced versus aHSCs. (B) Experimental design: qHSCs were seeded overnight on collagen type I-coated glass plates and then stimulated with TGF- $\beta$ 1  $\pm$  hSAP. (C) Col-GFP-positive area was calculated as a percent. Representative images are  $\times$ 20 magnification. (D) Total number of HSCs was estimated by Vitamin A expression (Vit.A $^+$ , considered as 100%). The number of Col-GFP $^+$ Vit.A $^+$  aHSCs/myofibroblasts was calculated as a percent of total Vit.A $^+$  cells. (E) Expression of  $\alpha$ -SMA and Col- $\alpha$ 1(I) mRNA levels was analyzed using quantitative RT-PCR (mRNA levels normalized by 18s). Data are mean  $\pm$  SD; \* $p$  < 0.05, \*\* $p$  < 0.03, \*\*\* $p$  < 0.01, Unpaired Student  $t$  test, one-way ANOVA. Abbreviations: aHSC, activated hepatic stellate cell; CCl $_4$ , carbon tetrachloride; hSAP, human serum amyloid P; qHSC, quiescent hepatic stellate cell; RT-PCR, reverse transcription polymerase chain reaction.

described.<sup>[11]</sup> Here, we explored whether hSAP can directly suppress the fibrogenic activation of HSCs.

### hSAP inhibited in vitro TGF $\beta$ 1-induced HSC activation

Purified quiescent HSCs ( $1 \times 10^5$  cells) were seeded on collagen type I-coated glass slides for 18 hours and then stimulated with TGF $\beta$ 1 (2 ng/mL for 72 h) in the presence or absence of different concentrations of hSAP (20, 30, and 40  $\mu$ g/mL, Figure 5B). Activation of Vitamin A $^+$  HSCs was visualized by upregulation of Col-GFP expression (Figure 5C). Immunofluorescent analysis revealed that TGF $\beta$ 1 stimulation + vehicle (PBS) induced rapid upregulation of Col-GFP expression in Vitamin A $^+$  qHSCs undergoing activation into aHSCs/myofibroblasts (in  $62 \pm 2\%$  of Col-GFP $^+$ VitA $^+$  HSCs vs. all Vit.A $^+$  HSCs considered as 100%, Figure 5D). In contrast, activation of qHSCs was inhibited in the presence of hSAP in a dose-dependent manner, as shown by the overall decrease of the fluorescent GFP signal (Figure 5C), as well as the reduced number of total Col-GFP $^+$ Vit.A $^+$  aHSCs in hSAP-treated TGF $\beta$ 1-stimulated aHSCs (vs. TGF $\beta$ 1-stimulated aHSCs, Figure 5D). The most significant suppression of collagen type I expression by  $\downarrow 45 \pm 5\%$  was observed in TGF $\beta$ 1-stimulated aHSCs treated with 40  $\mu$ g/mL of hSAP (compared to HSCs stimulated with TGF- $\beta$ 1 alone, Figures 5C, D). In accord, expression of Col1a1 and  $\alpha$ SMA mRNA was also suppressed by  $\downarrow 35 \pm 2\%$  in TGF- $\beta$ 1 + hSAP (40  $\mu$ g/mL)-treated HSCs (Figure 5E), indicating that treatment with hSAP prevents TGF $\beta$ 1-induced HSC activation in vitro. The concentration of 40  $\mu$ g/mL hSAP was chosen for the next study.

### hSAP inhibited in vitro ECM-mediated HSC activation

In addition to TGF $\beta$ 1, a stiff microenvironment activates HSCs.<sup>[22]</sup> The potential effect of hSAP on stiff matrix-induced HSC activation and proliferation was tested using the platform technology as described.<sup>[19]</sup> Briefly, 2

different kinds of ECM proteins were printed on the glass platforms onto which HSCs were seeded. qHSCs were isolated from naïve Col-GFP mice, seeded on ECM1 (composed of Fibronectin + Col1a1) and ECM2 (Fibronectin + Col1a3), and cultured for 6 days in a medium containing 10% FBS (which stimulates HSC activation and proliferation)  $\pm$  hSAP (40  $\mu$ g/mL, Figure 6A). As a control, quiescent HSCs were cultured in 1% FBS medium (lacking TGF $\beta$ 1 and growth factors). The activation of qHSCs was monitored by the upregulation of Col-GFP in cells using bright-field and fluorescent microscopy. Total cells were counted using Hoechst staining (Figure 6A).

Strong upregulation of GFP was observed in only HSC cultured for 6 days in ECM1 and ECM2 supplemented with 10% FBS (Figure 6A). As expected, qHSCs cultured in ECM1 or ECM2 + 1% FBS failed to activate, as shown by the lack of GFP upregulation in these cells (Figure 6A). Treatment with hSAP (40  $\mu$ g/mL) strongly decreased the number of GFP $^+$ -aHSCs cultured in ECM1 or ECM2 + 10% FBS without affecting cell viability. The number of GFP $^+$  HSCs per condition was calculated as a percent (vs. total HSCs visualized by Hoescht staining, considered as 100%). hSAP reduced the number of GFP $^+$  HSCs by  $\downarrow 66 \pm 3\%$  and  $\downarrow 63 \pm 5\%$  in ECM1 and ECM2 + 10% FBS cultures, respectively (compared to ECM1 and ECM2 + 10% FBS cultured HSCs, Figure 6B).

### hSAP inhibited in vitro TGF $\beta$ 1-mediated activation of human qHSCs

We tested if hSAP can exert a similar inhibitory effect on primary human qHSCs. Human qHSCs were isolated as described.<sup>[20]</sup> TGF $\beta$ 1-induced activation of qHSCs into myofibroblasts was suppressed in the presence of hSAP, as shown by the strong downregulation of TIMP1 ( $\downarrow 97 \pm 4\%$ ), DESMIN ( $\downarrow 66 \pm 3\%$ ),  $\alpha$ SMA ( $\downarrow 67 \pm 2\%$ ), VIMENTIN ( $\downarrow 75 \pm 3\%$ ), and COL1A1 ( $\downarrow 25 \pm 4\%$ ) (Figure 7A). In addition, we tested if hSAP can produce a cytotoxic effect on primary human hepatocytes.<sup>[18]</sup> Culturing of human hepatocytes in the presence of different concentrations of hSAP did not affect hepatocyte viability (as shown by the staining with Trypan Blue), albumin mRNA expression, or albumin



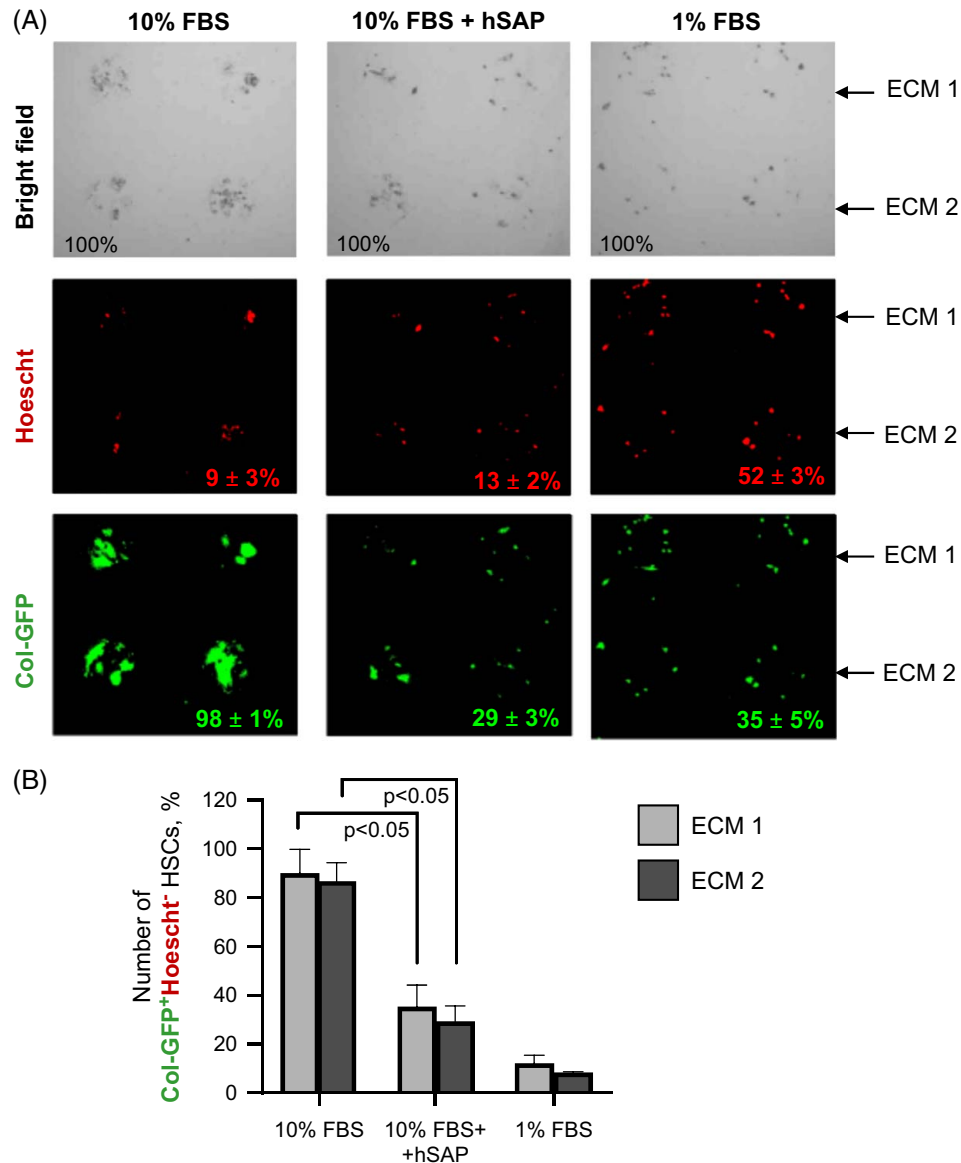


**FIGURE 6** Matrix-induced in vitro activation of qHSCs into myfibroblasts is inhibited in the presence of hSAP. (A) qHSCs were isolated from naïve Col-GFP mice and cultured on stiff ECM matrix (ECM1 and ECM2) and cultured in 1% FBS or 10% FBS ± hSAP (40 µg/mL) for 6 days. Expression of collagen type I was visualized by the upregulation of GFP in HSCs. Total cells were visualized by Hoescht staining. Representative bright-field and fluorescent images were ×4 magnification. (B) Activation of live Col-GFP<sup>+</sup> aHSC/myofibroblasts per condition was quantified as a percent compared to the total HSCs (100%). Data are mean ± SD; \* $p < 0.05$ , \*\* $p < 0.03$ , \*\*\* $p < 0.01$ . unpaired Student *t* test, one-way ANOVA. Abbreviations: aHSC, activated hepatic stellate cell; ECM, extracellular matrix; FBS, fetal bovine serum; hSAP, human serum amyloid P; qHSC, quiescent hepatic stellate cell.

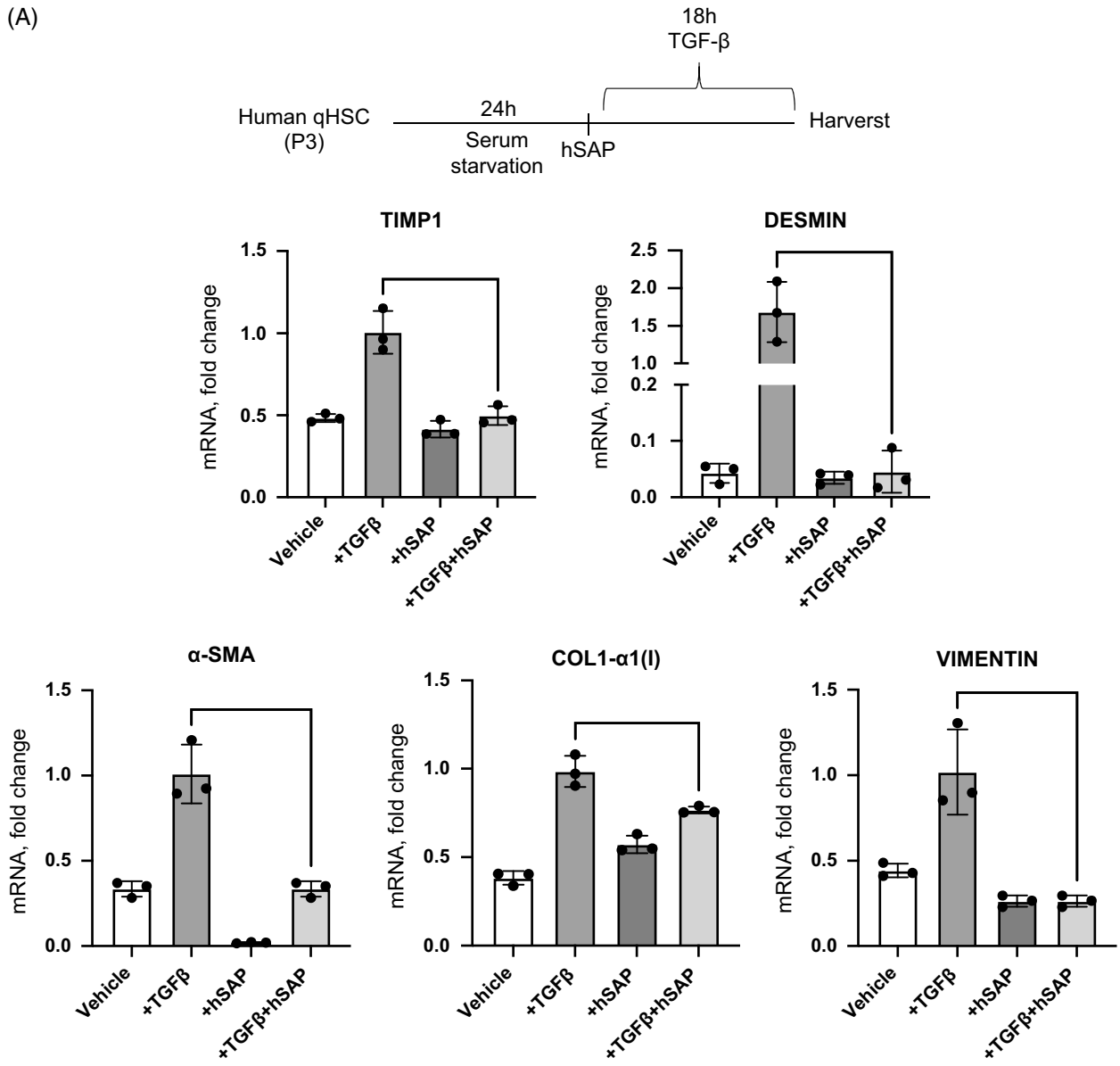
secretion, indicating that hSAP does not affect parenchymal liver cells (Supplemental Figure S4, <http://links.lww.com/HC9/B59>). Overall, our data suggest that hSAP can inhibit the activation of both fibrocytes and HSCs into myfibroblasts (Figure 7B).

## DISCUSSION

We assessed the effect of hSAP on the pathogenesis of liver fibrosis of different etiologies, BDL-induced liver fibrosis, which recapitulates a model for secondary

biliary fibrosis, and CCl<sub>4</sub>-induced liver fibrosis, which mimics postnecrotic toxic fibrosis. We demonstrated that prophylactic and therapeutic administration of hSAP mediated hepatoprotective, anti-inflammatory, and antifibrotic effects in BDL and CCl<sub>4</sub>-injured mice. hSAP has been implicated in the regulation of monocyte differentiation into fibrocytes and fibrocyte activation.<sup>[11]</sup> The current study focused on the potential effect of hSAP on the activation of fibrocytes and HSCs into myfibroblasts in the injured liver. We demonstrate that hSAP inhibits fibrocyte and HSC activation into collagen type I-producing myfibroblasts. Treatment with hSAP

(A)



(B)

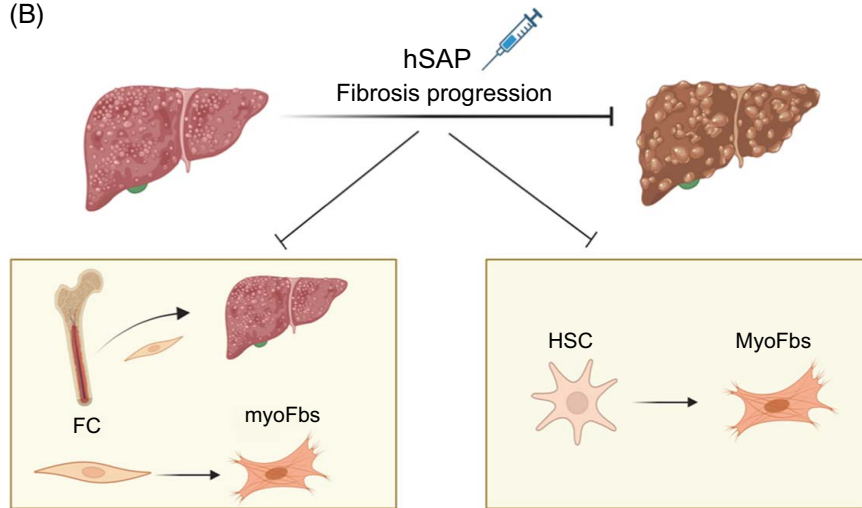


**FIGURE 7** In vitro activation of human HSCs into myofibroblasts is inhibited in the presence of hSAP. (A) Human HSC were isolated, starved, and pretreated with hSAP (1  $\mu\text{g}/\text{mL}$ , 15 min) followed by TGF $\beta$  stimulation (5 ng/mL, 18 h). Expression of fibrogenic markers (Timp1, Desmin,  $\alpha$ -SMA, Col- $\alpha$ 1(I), and Vimentin) was analyzed in hSAP- human HSCs  $\pm$  TGF $\beta$  using quantitative RT-PCR (mRNA fold change, normalized by 18s). Data are mean  $\pm$  SD; \* $p$  < 0.05, \*\* $p$  < 0.03, \*\*\* $p$  < 0.01, one-way ANOVA. (B) Schematic representation of hSAP targeting activation of FC and qHSCs activation into myofibroblasts (MyoFbs). Figure created using BioRender. Abbreviations: FC, fibrocyte; hSAP, human serum amyloid P; qHSC, quiescent hepatic stellate cell; RT-PCR, reverse transcription polymerase chain reaction.

may become a novel strategy for the treatment of liver fibrosis.

SAP exerts its functions through binding to Fc $\gamma$ RI and/or Fc $\gamma$ RIIa,<sup>[23]</sup> triggering downregulation of inflammatory responses in fibrocytes and monocytes.<sup>[24]</sup> It has been suggested that hSAP binds a polysaccharide receptor C-type lectin DC-SIGN on fibrocytes and monocytes.<sup>[25]</sup> hSAP also binds to misfolded proteins and multiple plasma proteins such as the complement component C1q and mannose-binding lectin to promote phagocytosis.<sup>[26]</sup> Using 9 different animal models, SAP inhibits the monocyte differentiation into fibrocytes. hSAP prevents fibrocyte-induced angiogenesis and fibrocyte differentiation into myofibroblasts.<sup>[11]</sup> We can speculate that binding of hSAP to Fc $\gamma$ R on fibrocytes prevents cytoskeletal rearrangements critical for their homing to the injured liver. Pilling et al first demonstrated that SAP suppresses the differentiation of monocytes into fibrocytes.<sup>[11]</sup> SAP binding to Ca<sup>2+</sup>-dependent ligands promotes subsequent Fc $\gamma$ R-dependent SAP-mediated inhibition of monocyte-to-fibrocyte differentiation, which was shown to be dependent on Src family kinase signaling.<sup>[24]</sup> Ligand-receptor complexes can be internalized by monocytes/fibrocytes, and this internalization can attenuate or terminate the signaling through the degradation of the involved proteins.<sup>[27]</sup> Thus, hSAP-opsonized apoptotic cells were shown to inhibit the monocyte activation into fibrocytes and suppress the expression of IL-6 and Pdgfb.<sup>[24]</sup> It was unknown if hSAP can affect the activation of myofibroblasts of nonfibrocyte origin.

Although BDL and CCl<sub>4</sub> induce liver fibrosis by activating different cellular pathways, inflammatory monocytes, fibrocytes, and fibrogenic aHSCs play a key role in the pathogenesis of liver fibrosis of different etiologies. Remarkably, hSAP suppressed inflammation and fibrosis in both models through multiple mechanisms.

Macrophages promote activation of HSCs during fibrosis progression through the release of paracrine factors, including TGF- $\beta$ 1.<sup>[1]</sup> Blocking macrophage infiltration or depletion of myeloid populations inhibits the activation of fibrocytes and HSCs, blunting liver fibrosis.<sup>[28,29]</sup> Our present study demonstrated that hSAP administration reduced the accumulation of F4/80<sup>+</sup> and CD68<sup>+</sup> macrophages in the livers of BDL-injured and CCl<sub>4</sub>-injured mice. Our findings are consistent with the previously reported therapeutic effect of hSAP on experimental models of pulmonary and kidney fibrosis

due to reduced infiltration and activation of macrophages in the injured organ. hSAP was shown to trigger the downregulation of inflammatory responses in activated monocytes and macrophages.<sup>[24]</sup> Similarly, using models of BDL and CCl<sub>4</sub>-induced liver fibrosis, our study demonstrated that mRNA levels of proinflammatory factors, such as IL-1 $\beta$ , IL-6, and TNF $\alpha$ , were significantly reduced in hSAP-treated mice, and this effect was associated with inhibition of macrophage activation. Previous studies implicated hSAP in the suppression of inflammatory responses in monocytes, myeloid cells, and fibrocytes.<sup>[11]</sup> Here, we demonstrate that hSAP inhibits fibrocyte homing to the liver and spleen, as well as fibrocyte differentiation into myofibroblasts. In addition, hSAP can directly act on HSCs and attenuate their activation. The relative contribution of hSAP functions in different cell types to the suppression of liver fibrosis remains to be clarified.

Cultured fibrocytes can differentiate into myofibroblasts in response to TGF- $\beta$ 1, and this effect was shown to be abrogated by hSAP.<sup>[11]</sup> Fibrocytes also secrete growth factors and cytokines, such as TGF- $\beta$ 1 and MCP-1, which promote deposition of ECM in the local area of fibrosis.<sup>[11]</sup> In BDL-induced liver fibrosis, fibrocytes migrate to the injured liver, reside in a portal area in close proximity to HSCs and inflammatory cells, and constitute 6%–8% of all collagen type I-producing cells. Although fibrocytes do not represent a major population of collagen type I-producing cells,<sup>[30]</sup> they seem to be a pre-requisite component of liver fibrosis. Based on the in vivo study using Col-GFP mice after BDL, here we demonstrate that hSAP inhibited the migration of fibrocytes from BM to the injured liver. To test whether hSAP could suppress the differentiation of fibrocytes in vitro, fibrocytes were isolated from Col-GFP mice and cultured with TGF- $\beta$ 1. hSAP suppressed the differentiation of fibrocytes into myofibroblasts. Together, these data demonstrate that hSAP treatment suppresses fibrocyte recruitment and activation.

Most liver myofibroblasts arise from the activation of qHSCs. In response to injury, qHSCs undergo morphological and functional changes, lose Vitamin A expression, and activate myofibroblasts.<sup>[1]</sup> In BDL and CCl<sub>4</sub>-injured mice, the percentage of  $\alpha$ -SMA and Desmin-positive cells was significantly reduced following hSAP treatment (compared to controls). This effect can be attributed to reduced inflammation or the direct effect of hSAP on HSCs. We tested if hSAP can directly inhibit the activation of qHSCs. TGF $\beta$ 1- and/or stiff

matrix-induced activation of freshly isolated primary quiescent mouse HSCs into myofibroblasts was suppressed in the presence of hSAP in a dose-dependent manner. Our data demonstrate that hSAP has a direct inhibitory effect on the activation of quiescent HSCs in vitro. In support, treatment with hSAP inhibits TGF $\beta$ -induced activation of human qHSCs. These data provide important evidence for translational research, suggesting that administration of hSAP can ameliorate liver fibrosis of different etiologies through targeting cells of different origins, such as myeloid and mesenchymal cells. We can speculate that Fc $\gamma$ RI receptors may play a similar role in HSC activation through the regulation of HSC differentiation and proliferation. The binding of hSAP to Fc $\gamma$ RI might regulate Lck expression and activation of HSCs. In accord, Lck was implicated in the regulation of Smas2/3 and Stat3 signaling in fibroblast-like cells.<sup>[31]</sup>

Despite extensive investigation of hSAP/PTX2-fibrocyte interaction,<sup>[11,15]</sup> the interest in the role of hSAP in wound healing was hampered due to the confusion with SAP component,<sup>[32]</sup> which exacerbates amyloidosis in patients, and the depletion of SAP component is successfully used to treat these patients.<sup>[33]</sup> Unlike the SAP component, hSAP/PTX2 exhibits antifibrotic properties.<sup>[11]</sup> hSAP is produced by hepatocytes and secreted into the blood. Serum levels of SAP are maintained between 30 and 50  $\mu$ g/mL in humans and mice.<sup>[21]</sup> Compared to healthy individuals, serum levels of SAP are downregulated in patients with renal fibrosis, pulmonary fibrosis, scleroderma, myelofibrosis, and rheumatoid arthritis, suggesting the role of SAP deficiency in contributing to the fibrosis.<sup>[11,21]</sup> Therefore, reconstitution of serum levels of SAP may be therapeutic in patients with fibrogenic diseases. Injections of recombinant human SAP/PTX2 (also listed as PRM-151)<sup>[34]</sup> improved lung function in a phase Ib trial and a phase II trial in patients with pulmonary fibrosis.<sup>[35,36]</sup> In the 28-week phase II trial, SAP injections slowed the decline in forced exhalation volume and prevented the decline in the distance patients could walk. Moreover, in a 27-patient phase II trial in myelofibrosis, administration of SAP reduced fibrosis and improved BM function.<sup>[11]</sup> Thus, hSAP may become a treatment of choice or a part of multitarget therapy for liver fibrosis of different etiologies.

## AUTHOR CONTRIBUTIONS

Min Cong designed and performed experiments, analyzed data, and wrote the manuscript; Raquel Carvalho Gontijo Weber, Sadatsugu Sakane, Vivian Zhang, Chunyan Jiang, Kojiro Taura, Yuzo Kodama, Samuele DeMinicis, Souradipta Ganguly, and David Brafman performed experiments and collected data; Shu Chien, Michael Kramer, and Mark Lupher designed experiments, provided hSAP, and support; David A. Brenner provided support, and helped with the manuscript

preparation; Jun Xu helped with the manuscript preparation; and Tatiana Kisseleva designed the study, provided support, and wrote the manuscript.

## FUNDING INFORMATION

This research was supported by the National Institutes of Health R01DK111866, R56DK088837, DK099205, AA028550, DK101737, AA011999, DK120515, AA029019, DK091183, P42ES010337, and R44DK115242 (Tatiana Kisseleva and David Brafman).

## CONFLICTS OF INTEREST

Jun Xu is employed by and owns stock in Gilead Sciences Incorporated. Mark Lupher owns stock in Roche. The remaining authors have no conflicts to report.

## REFERENCES

1. Kisseleva T, Brenner D. Molecular and cellular mechanisms of liver fibrosis and its regression. *Nat Rev Gastroenterol Hepatol.* 2021;18:151–66.
2. Friedman SL. Liver fibrosis—From bench to bedside. *J Hepatol.* 2003;38(suppl 1):S38–53.
3. Quan TE, Cowper S, Wu SP, Bockenstedt LK, Bucala R. Circulating fibrocytes: Collagen-secreting cells of the peripheral blood. *Int J Biochem Cell Biol.* 2004;36:598–606.
4. Phillips RJ, Burdick MD, Hong K, Lutz MA, Murray LA, Xue YY, et al. Circulating fibrocytes traffic to the lungs in response to CXCL12 and mediate fibrosis. *J Clin Invest.* 2004;114:438–46.
5. Hashimoto N, Jin H, Liu T, Chensue SW, Phan SH. Bone marrow-derived progenitor cells in pulmonary fibrosis. *J Clin Invest.* 2004;113:243–52.
6. Galan A, Cowper SE, Bucala R. Nephrogenic systemic fibrosis (nephrogenic fibrosing dermopathy). *Curr Opin Rheumatol.* 2006;18:614–7.
7. Kisseleva T, Brenner DA. Fibrogenesis of parenchymal organs. *Proc Am Thorac Soc.* 2008;5:338–42.
8. Abe R, Donnelly SC, Peng T, Bucala R, Metz CN. Peripheral blood fibrocytes: Differentiation pathway and migration to wound sites. *J Immunol.* 2001;166:7556–62.
9. Kisseleva T, von Köckritz-Blickwede M, Reichart D, McGillvray SM, Wingender G, Kronenberg M, et al. Fibrocyte-like cells recruited to the spleen support innate and adaptive immune responses to acute injury or infection. *J Mol Med (Berl).* 2011;89:997–1013.
10. Crawford JR, Pilling D, Gomer RH. Improved serum-free culture conditions for spleen-derived murine fibrocytes. *J Immunol Methods.* 2010;363:9–20.
11. Pilling D, Gomer RH. The development of serum amyloid P as a possible therapeutic. *Front Immunol.* 2018;9:2328.
12. Hohenester E, Hutchinson WL, Pepys MB, Wood SP. Crystal structure of a decameric complex of human serum amyloid P component with bound dAMP. *J Mol Biol.* 1997;269:570–8.
13. Balmelli C, Alves MP, Steiner E, Zingg D, Peduto N, Ruggli N, et al. Responsiveness of fibrocytes to toll-like receptor danger signals. *Immunobiology.* 2007;212:693–9.
14. Pilling D, Roife D, Wang M, Ronkainen SD, Crawford JR, Travis EL, et al. Reduction of bleomycin-induced pulmonary fibrosis by serum amyloid P. *J Immunol.* 2007;179:4035–44.
15. Herzog EL, Bucala R. Fibrocytes in health and disease. *Exp Hematol.* 2010;38:548–56.
16. Yata Y, Scanga A, Gillan A, Yang L, Reif S, Breindl M, et al. DNase I-hypersensitive sites enhance alpha1(I) collagen gene



- expression in hepatic stellate cells. *Hepatology*. 2003;37:267–76.
17. Seki E, De Minicis S, Österreicher CH, Kluwe J, Osawa Y, Brenner DA, et al. TLR4 enhances TGF-beta signaling and hepatic fibrosis. *Nat Med*. 2007;13:1324–32.
  18. Liu X, Lam K, Zhao H, Sakane S, Kim HY, Eguileor A, et al. Isolation of primary human liver cells from normal and nonalcoholic steatohepatitis livers. *STAR Protoc*. 2023;4:102391.
  19. Brafman DA, de Minicis S, Seki E, Shah KD, Teng D, Brenner D, et al. Investigating the role of the extracellular environment in modulating hepatic stellate cell biology with arrayed combinatorial microenvironments. *Integr Biol (Camb)*. 2009;1:513–24.
  20. Liu X, Brenner DA, Kisseleva T. Human hepatic stellate cells: Isolation and characterization. *Methods Mol Biol*. 2023;2669:221–32.
  21. Pilling D, Buckley CD, Salmon M, Gomer RH. Inhibition of fibrocyte differentiation by serum amyloid P. *J Immunol*. 2003;171:5537–46.
  22. Wells RG. The role of matrix stiffness in regulating cell behavior. *Hepatology*. 2008;47:1394–400.
  23. Crawford JR, Pilling D, Gomer RH. FcγRI mediates serum amyloid P inhibition of fibrocyte differentiation. *J Leukoc Biol*. 2012;92:711.
  24. Castano AP, Lin SL, Surowy T, Nowlin BT, Turlapati SA, Patel T, et al. Serum amyloid P inhibits fibrosis through FcγR-dependent monocyte-macrophage regulation in vivo. *Sci Transl Med*. 2009;1:5ra13.
  25. Cox N, Pilling D, Gomer RH. DC-SIGN activation mediates the differential effects of SAP and CRP on the innate immune system and inhibits fibrosis in mice. *Proc Natl Acad Sci USA*. 2015;112:8385–90.
  26. Kilpatrick DC. Isolation of human mannan binding lectin, serum amyloid P component and related factors from Cohn fraction III. *Transfus Med*. 1997;7:289–94.
  27. Benadda S, Nogue M, Koumantou D, Bens M, De Luca M, Pellé O, et al. Activating FcγRI function depends on endosomal-signaling platforms. *iScience*. 2023;26:107055.
  28. Imamura M, Ogawa T, Sasaguri Y, Chayama K, Ueno H. Suppression of macrophage infiltration inhibits activation of hepatic stellate cells and liver fibrogenesis in rats. *Gastroenterology*. 2005;128:138–46.
  29. Duffield JS, Forbes SJ, Constandinou CM, Clay S, Partolina M, Vuthoori S, et al. Selective depletion of macrophages reveals distinct, opposing roles during liver injury and repair. *J Clin Invest*. 2005;115:56–65.
  30. Kleaveland KR, Velikoff M, Yang J, Agarwal M, Rippe RA, Moore BB, et al. Fibrocytes are not an essential source of type I collagen during lung fibrosis. *J Immunol*. 2014;193:5229–39.
  31. Shen H, Zhang M, Kaita K, Minuk GY, Rempel J, Gong Y. Expression of Fc fragment receptors of immunoglobulin G (FcγRs) in rat hepatic stellate cells. *Dig Dis Sci*. 2005;50:181–7.
  32. Steel DM, Whitehead AS. The major acute phase reactants: C-reactive protein, serum amyloid P component and serum amyloid A protein. *Immunol Today*. 1994;15:81–8.
  33. Richards DB, Cookson LM, Barton SV, Liefwaard L, Lane T, Hutt DF, et al. Repeat doses of antibody to serum amyloid P component clear amyloid deposits in patients with systemic amyloidosis. *Sci Transl Med*. 2018;10:eaa3128.
  34. Duffield JS, Luper ML Jr. PRM-151 (recombinant human serum amyloid P/pentraxin 2) for the treatment of fibrosis. *Drug News Perspect*. 2010;23:305–15.
  35. Dillingh MR, van den Blink B, Moerland M, van Dongen MGJ, Levi M, Kleinjan A, et al. Recombinant human serum amyloid P in healthy volunteers and patients with pulmonary fibrosis. *Pulm Pharmacol Ther*. 2013;26:672–6.
  36. Raghu G, van den Blink B, Hamblin MJ, Brown AW, Golden JA, Ho LA, et al. Effect of Recombinant human pentraxin 2 vs placebo on change in forced vital capacity in patients with idiopathic pulmonary fibrosis: A randomized clinical trial. *JAMA*. 2018;319:2299–307.

**How to cite this article:** Cong M, Carvalho Gontijo Weber R, Sakane S, Zhang V, Jiang C, Taura K, et al. Serum amyloid P (PTX2) attenuates hepatic fibrosis in mice by inhibiting the activation of fibrocytes and HSCs. *Hepatol Commun*. 2024;8:e0557. <https://doi.org/10.1097/HC9.0000000000000557>